Approximately analytical model for inner-shell photoionization x-ray lasers in low-*Z* elements

Jiansheng Liu,[1,2] Ruxin Li,[1] Zhizhan Xu,[1] and Jingru Liu[2]
[1]*Shanghai Institute of Optics and Fine Mechanics, Chinese Academy of Sciences, P. O. Box 800-211, Shanghai 201800, People's Republic of China, and* [2]*Northwest Institute of Nuclear Technology, P. O. Box 69, Xian 710024, People's Republic of China*

(Received 28 January 2000; revised manuscript received 25 August 2000; published 12 February 2001)

A model employing five energy levels and a fit linear rising photopumping rate of x-ray source is proposed to analyze the gain of inner-shell photoionization (ISPI) x-ray lasers when the lasing medium is irradiated with a filtered approximate blackbody source. The deduced analytical expressions for the time of the onset of the peak gain and its peak value reveal the effects of Auger decay, electron-impact ionization, the density of lasing medium, and the increase rate of pumping rate on the duration and the peak value of the laser gain. Also the requirements on the intensity of the driving ultrashort pulse laser can be estimated. The model is generally suitable for analyzing ISPI x-ray lasers in low-*Z* elements from carbon to neon although carbon is analyzed in details as a representative to verify the validity of the model. $K\alpha$ x-ray lasing at 3.2 nm in nitrogen is also discussed as an attractive candidate for experimentally implementing a ''water window'' ISPI x-ray laser.

DOI: 10.1103/PhysRevA.63.033809 PACS number(s): 42.55.Vc, 32.80.Hd, 52.25.Os, 52.38.−r

I. INTRODUCTION

The last decade of the last millennium has witnessed the rapid advances in obtaining high optical intensity through chirped pulse amplification (CPA) which has led to the generation of ultrashort pulse (USP) lasers with durations as short as 20 fs and powers >1 PW [1,2]. The developing optical parameter CPA scheme has the potential to produce USP lasers with shorter duration and higher power. The so-called ''table-top'' terawatt (T^3) laser systems, which have high repetition rates of 10 HZ or higher as well as a much lower cost compared to the large systems, can now be obtained in many laboratories in the world. Until now, a great amount of exciting work has been done in many fields such as high-order harmonics generation (HHG), electron acceleration, x-ray lasing at short wavelength near the ''water window'' (2.3–4.4 nm) through electron collisionally pumped scheme [3], nuclear reaction in atom clusters [4], etc. Experiments in material science have shown that the coherent or incoherent x-ray source with short pulse duration (<100 fs) can find many applications in biochemistry, microphysics, microelectronics, microlithography, and so on. In the past 10 years, the considerable progress in laser driven x-ray lasers has brought the wavelength of x-ray lasers down to the ''water window'' through an electron collisionally pumped scheme. But it seems difficult to produce x-ray laser at shorter wavelength (<2 nm) with the present schemes. The same problem existed in HHG owing to its difficulty in phase matching and low conversion efficiency at short wavelengths [5].

X-ray pumped inner-shell photoionization (ISPI) x-ray laser is now a very attractive approach to short-wavelength lasing (<5 nm) with short pulse duration (<50 fs). It was originally proposed by Duguay and Rentzepis [6] that ISPI can produce population inversion since the inner-shell electrons in atoms have a much larger photoionization cross section than the outer-shell electrons when the energy of photons is above the *K*-shell ionization potential. But the problems of electron-impact ionization of the ground state along with Auger decay of the *K*-shell holes make this scheme very difficult to be realized, and the most critical requirement is to have a highly intense x-ray source with a short rise time. Nevertheless, the advances in ultrashort pulse laser technology will change this situation. More recent work using an approximate blackbody source reported by Kapteyn *et al.* [7–11] concentrated on a $K\alpha$ laser in neon (1.5 nm) where x-ray lasing has not been demonstrated because the intensity of the x-ray source is not sufficient. Tajima *et al.* proposed a new lasing mechanism of ultrafast x-ray process with hollow atoms using Larmor radiation [12], which requires an ultraintense ultrashort pulse laser ($>10^{19}$ W/cm^2). Using a conventional ISPI scheme, Moon and Eder [13] presented their simulation results of $K\alpha$ x-ray lasing at 4.5 nm in carbon and indicated that the now available ultrashort pulse laser (1 J, 40 fs) is sufficient to yield a net effective gain length product GL of 10, at saturation when GL is 18, an output of 0.1 μJ per pulse would be expected. However, their analysis for the ISPI x-ray laser scheme was dependent on the complicated numerical codes and it is not convenient for one to analyze the laser gain and select optimum parameters. Moreover, the laser gains in carbon are significantly over estimated in the work of Moon and Eder [13].

In this paper, we discuss the ISPI x-ray lasing scheme in low *Z* elements from carbon to neon. A new model employing five energy levels and a fit linear rising pumping rate of x-ray source is proposed to analyze the gain of ISPI x-ray lasers when the lasing medium is irradiated with a filtered approximate blackbody source. The model is generally suitable to ISIP x-ray lasers in low *Z* elements from carbon to neon although carbon is analyzed in detail as a representative to verify the validity of the model. The calculated results by using the analytical expressions agree well with the numerical simulations. Moreover, $K\alpha$ x-ray lasing at 3.2 nm in nitrogen is also discussed as an attractive candidate for experimentally implementing a ''water window'' ISPI x-ray laser.

This paper is structured in the following way. In Sec. II we describe the model and present the results of numerical

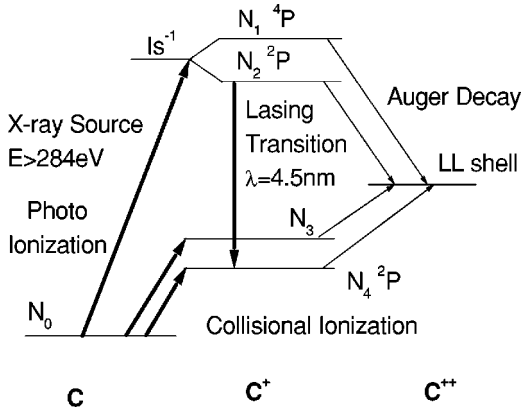

FIG. 1. Energy-level diagram for inner-shell photoionization x-ray lasing in carbon at 4.5 nm.

simulations. In Sec. III we describe an analytical model and present calculated results based on the model. In Sec. IV we discuss the calculated results. In Sec. V we analyze the ISPI x-ray laser in nitrogen and we summarize this work in the final section.

II. MODEL AND NUMERICAL SIMULATIONS

Shown in Fig. 1 is the five-energy level scheme for *K*-shell photoionization x-ray lasing in carbon. An x-ray source creates a *K*-shell hole in carbon atom and then an allowed $K\rightarrow L(1s^{-1}\rightarrow 2p^1)$ radiative transition can take place yielding a photon of 273 eV. For x-rays above the *K*-shell ionization energy (284 eV), the photoionization cross section of *K* shell is more than 20 times that of *L* shell. Therefore the population inversion between *K*- and *L*-shell holes is possible to obtain. However, the major obstacle is that the *K*-shell holes undergo a very fast nonradiative decay, which almost simultaneously produces deleterious second electrons. The lifetime of Auger decay is 10.3 fs compared to the radiative transition lifetime of 2930 fs [14], so the fluorescence efficiency is very low. On the other hand, the free electrons produced by the photo- and electron-impact ionization will unavoidably ionize the neutral atoms to populate the lower laser states and quench the laser gain. The x-ray pumping source therefore must have a fast rise time to achieve significant population inversion before electron-impact ionization destroys the inversion. In order to examine the processes more directly, a new model considering five-energy level and a fit linear rising pumping rate of x-ray source is proposed to analyze the laser gain when the lasing medium is irradiated with a filtered approximate blackbody source.

The ground state of neutral carbon atom is $1s^2 2s^2 2p^2(N_0,{}^3P)$, the removal of one $1s$ electron gives $1s^{-1}2s^2 2p^2$ with 2 states (quartet, ${}^4P$) N_1 and (doublet, ${}^2P$) N_2. The lasing transition is the allowed transition of a $2p$ electron into the $1s$ hole to form the $1s^2 2s^2 2p^1({}^2P,N_4)$ ionized carbon ground state. So only the ${}^2P$ upper state has an allowed transition to this lower laser state. Hence, only one third of the total x-ray pumping rate produces the upper laser state (N_2) and supports the lasing transition. $1s^2 2s^1 2p^2(2s^{-1})$ corresponds to another energy level (N_3) of C^+. In the calculation, the fast atomic processes such as photoionization, electron-impact ionization, Auger decay, and radiative transition are considered, while the effects of three-body recombination and autoionization can be negligible [9]. Therefore, the rate equations of the various energy levels, as illustrated in Fig. 1, may be written as follows:

$$\begin{aligned}
\dot{N}_0 &= -N_0(R_{01}^{e+P}+R_{03}^{e+P}+R_{04}^{e+P}),\\
\dot{N}_1 &= R_1 N_0 R_{01}^{e+P} - D_1 N_1,\\
\dot{N}_2 &= R_2 N_0 R_{01}^{e+P} - D_2 N_2,\\
\dot{N}_3 &= N_0 R_{03}^{e+P} - D_3 N_3,\\
\dot{N}_4 &= N_0 R_{04}^{e+P} - D_4 N_4,
\end{aligned} \tag{1}$$

where $R_{0n}^{e+P}=R_{0n}^{e}+R_{0n}^{P}$, $R_{0n}^{e}=\langle n_e\sigma_{e0n}v_e\rangle=n_e\langle\sigma_{e0n}v_e\rangle$, $R_{0n}^{P}=\int_{E_n}^{\infty} I\sigma_n(v)/h\upsilon\, dv$. R_{0n}^{P}, R_{0n}^{e} are the rate of photoionization and electron-impact ionization. The subscripts 0, 1, 2, 3, and 4 correspond to the five energy levels N_0, N_1, N_2, N_3, and N_4, respectively. The coefficient D_n expresses the decay rate of the state N_n, including photoionization and electron-impact ionization. For the state (N_1) and upper laser state (N_2), the Auger decay D_{a1}, D_{a2} is also included. $\sigma_n(v)$, E_n are the photoionization cross section and ionization energy of the N_n energy level, respectively. R_1, R_2 are the fractional ratio of x-ray pumping rate for the states N_1, N_2 and $R_1+R_2=1$. For carbon R_1 is 2/3 and R_2 is 1/3. Since the energy-level split of the upper states is considered, there would involve some correction of the Auger decay and radiative rate. The fluorescence yield $W_k=R_2A/(R_1D_{a1}+R_2D_{a2})=A(/2D_{a1}+D_{a2})$, D_{a1}, D_{a2} (which affects the linewidth of $K\alpha$ radiation) may be considered as the same $=(10.3\text{ fs})^{-1}$, therefore the radiative rate *A* increases three fold.

The rate equation (1) may be calculated through numerical simulations. X-ray pumping source is modeled as an approximate blackbody emitter of time-varying temperature with a thin x-ray high pass filter [9]. The blackbody emitter corresponds to the laser heated region, which probably is a thin layer of solid or structured material deposited onto the beryllium. The beryllium acts to absorb low-energy x rays that only produce outer-shell ionization of lasing medium. The temperature $T(t)$ of the blackbody that is used in the simulations is

$$T(t)=C\left[\int_{-\infty}^{t}\operatorname{sech}^2\left(1.76\frac{t'}{\tau}\right)dt'\right]^{4/9}, \tag{2}$$

where τ is the full width at half maximum of the USP laser that is assumed to have a sech^2 pulse shape. The x-ray source is then calculated by using the usual blackbody formula assuming an average emissivity of 0.1, which is expected to decrease as temperature increases. The unavoidable 25% attenuation of x rays above the *K* edge by the thin filter that is used to filter out the low-energy x rays is also considered, so the photopumping rate of the *K*-shell is given as

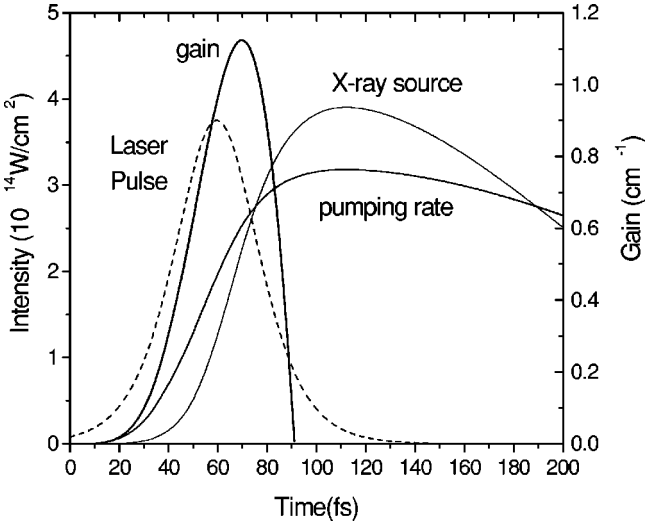

FIG. 2. The time-varying gain along with the filtered intensity of the x-ray source, the ultrashort pulse laser, and the pumping rate of *K* shell in carbon (an USP laser of 1 J, 40 fs).

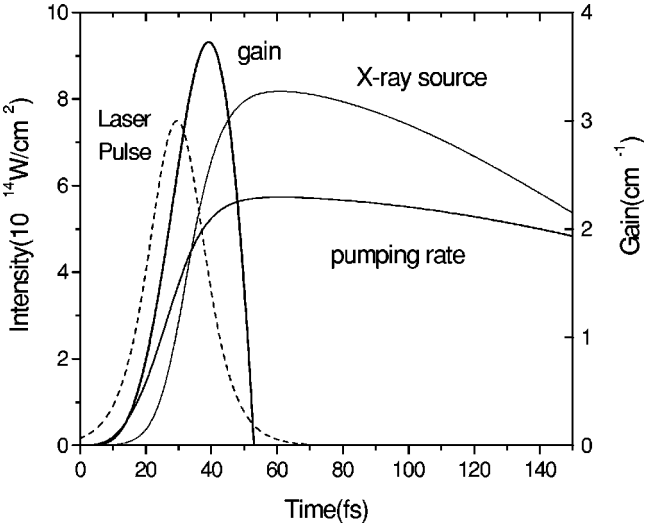

FIG. 3. The time-varying gain along with the filtered intensity of the x-ray source, the ultrashort pulse laser, and the pumping rate of *K* shell in carbon (an USP laser of 100 TW, 20 fs).

$$R_{01}^{P}=0.75\times\text{emissivity}\times\int_{\varepsilon}^{\infty}\frac{\sigma_K(v)}{hv}B(v)dv, \qquad (3)$$

where σ_K, ε are the photoionization cross section and ionization potential of *K* shell, respectively. Employing the analytical model of the laser heating of solids [17], a driving laser with an energy of 1 J, 40 fs is able to obtain a high dense plasma of 500 eV temperature when it is focused to a line 5 μm$\times$1 cm if the absorption of 30% is used. The model of Moon and Eder, in which a structured target is employed, may have a high absorption of 60%. But here in our simulations, the maximum temperature of 500 eV is used.

The gain of x rays from the lasing process by the transition between an upper state and a lower state is given by $G=\sigma_g(N_2-gN_4)$. $g=g_2/g_4$ ($=1$ for carbon) is the ratio of the statistical weights and σ_g is the stimulated emission cross section. The neutral atom density is set as 1.3×10^{19} cm^{-3} and the net peak gain is $\cong0.56$ cm^{-1} accounting for the absorption of 0.56 cm^{-1}. Figure 2 shows the laser gain as a function of time along with the USP laser, the filtered intensity of x-ray source and the pumping rate of *K* shell in carbon. If a current available USP laser of 100 TW, 20 fs [19] is employed, the neutral atom density may be set as 3.0×10^{19} cm^{-3} and a net peak gain of 2.4 cm^{-1} is able to be obtained. In Fig. 3, we show the laser gain as a function of time along with the USP laser, the filtered intensity of x-ray source, and the pumping rate of *K* shell in carbon.

III. ANALYTICAL MODEL AND CALCULATION

It can be seen from Fig. 2 and Fig. 3 that after the laser gain develops to its maximum, the pumping of x-ray source almost gives no contribution to the gain. Figure 4 shows that the photopumping rate of *K* shell is very close to a linear increase function of time during the rise time (which makes the major contribution to the laser gain). Considering the filtered x-ray pumping source, the majority of low-energy x rays has been absorbed so that the photoionization rate of *L* shell is very small compared to that of *K* shell, and the electron-impact ionization of neutral atoms makes the major contribution to the population of the lower laser states. We consider only the photoionization of *K* shell, Auger decay of *K*-shell hole, and the outer-shell electron-impact ionization of the ground state (although the numerical simulations shown in Sec. II do not make this assumption, the results are almost the same). Moreover, the photopumping rate of *K* shell as shown in Fig. 4 may be reasonably fitted as $R_{01}^{P}=R_pt$, R_p is the increase rate of pumping rate (IRPR). Based on the above considerations, the rate equation (1) may be simplified as follows:

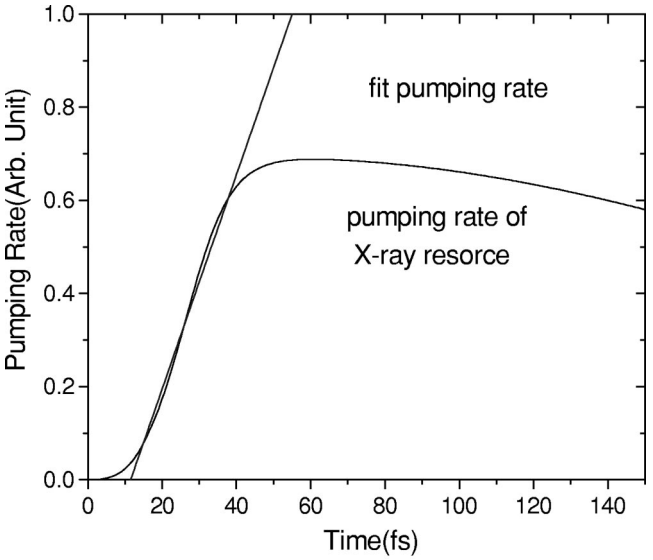

FIG. 4. The pumping rate of the x-ray source as a function of time compared to the fit pumping rate for the theoretical calculation.

$$\begin{aligned}
\dot{N}_0 &= -N_0(R_p t + R^e_{03} + R^e_{04}),\\
\dot{N}_1 &= R_1 N_0 R_p t - D_{a1} N_1,\\
\dot{N}_2 &= R_2 N_0 R_p t - D_{a2} N_2,\\
\dot{N}_3 &= N_0 R^e_{03} = N_0 n_e \langle \sigma_{e03} v_e \rangle,\\
\dot{N}_4 &= N_0 R^e_{04} = N_0 n_e \langle \sigma_{e04} v_e \rangle.
\end{aligned} \tag{4}$$

The population of N_0 in Eq. (4) may be expressed as

$$N_0 = N_{00} \exp\left(-\frac{1}{2} R_p t^2 - \int (R^e_{03} + R^e_{04}) dt \right) \cong N_{00}, \tag{5}$$

where N_{00} is the initial density of neutral C atoms. The carbon atom is less than 1% ionized during the time of the laser gain, which means that the depopulation of the ground state through photoionization and electron-impact ionization can be ignored compared to the population of the ground state. Therefore the population of the ground state N_0 can be treated as a constant $\cong N_{00}$. The population of N_1, N_2 in Eq. (4) may be analytically solved straightforward as follows:

$$\begin{aligned}
N_1 &= \frac{R_1 N_{00} R_p}{D^2_{a1}} (D_{a1} t + e^{-D_{a1} t} - 1),\\
N_2 &= \frac{R_2 N_{00} R_p}{D^2_{a2}} (D_{a2} t + e^{-D_{a2} t} - 1).
\end{aligned} \tag{6}$$

The electron density produced through the photoionization of *K* shell and Auger decay can be expressed as

$$n_{e1} = \int_0^t (N_0 R_p t' + D_{a1} N_{a1} + D_{a2} N_{a2}) dt' \tag{7}$$

and the total density of electron is given as

$$n_e = n_{e1} + N_3 + N_4. \tag{8}$$

Therefore, the population of the lower laser state may also be analytically solved. And then the laser gain is derived as

$$\begin{aligned}
G &= \sigma_g (N_2 - g N_4)\\
&= \sigma_g N_{00} R_2 R_p \left[g \frac{b}{a} t^2 + \left(\frac{a}{D_{a2} b} - \frac{g}{D_{a2}} + \frac{2g}{a} \right) \frac{b}{a} t \right.\\
&\quad \left. - g \frac{b}{a} \left(\frac{2}{a^2} - \frac{1}{a D_{a2}} \right) (e^{at} - 1) - \frac{1 - e^{-D_{a2} t}}{D^2_{a2}} \right]\\
&\quad + \sigma_g N_{00} R_1 R_p \left[g \frac{b}{a} t^2 + \left(-\frac{g}{D_{a1}} + \frac{2g}{a} \right) \frac{b}{a} t \right.\\
&\quad \left. - g \frac{b}{a} \left(\frac{2}{a^2} - \frac{1}{a D_{a1}} \right) (e^{at} - 1) \right],
\end{aligned} \tag{9}$$

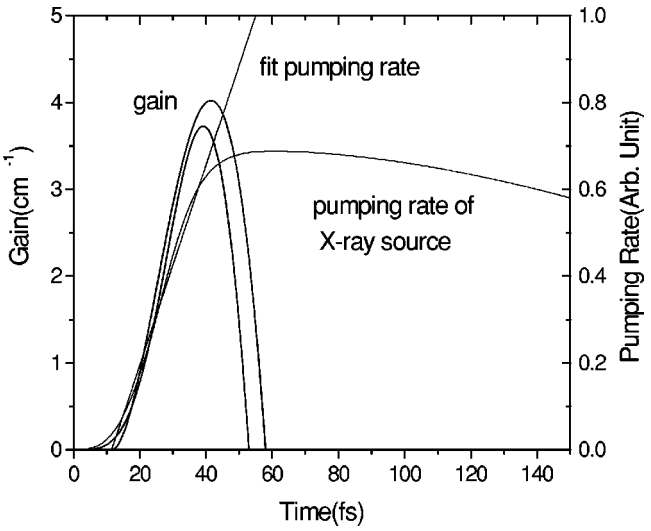

FIG. 5. The time-varying gain calculated via Eq. (9) compared to that of our simulations along with their pumping rate of *K* shell in carbon.

where $a = N_{00}\langle(\sigma_{e03} + \sigma_{e04}) v_e\rangle$, $b = N_{00}\langle \sigma_{e04} v_e \rangle$, $g = g_2 / g_4$, and the stimulated emission cross section $\sigma_g = \lambda^2 / 8\pi (4 \ln 2/\pi)^{1/2} A/\Delta v$. $\sigma_{e03,4}$ is the electron-impact ionization cross section of *L* shell and σ_{e03} is several times smaller than σ_{e04}, v_e is the thermal electron velocity, and g is the ratio of the statistical weights. If the above equation is differentiated with time t, the time t_{peak} for the onset of the peak gain can be obtained:

$$t_{peak} \cong \sqrt{\frac{R_2}{g D_{a2} b}} = \sqrt{\frac{R_2}{g D_{a2} N_{00} \langle \sigma_{e04} v_e \rangle}}, \tag{10}$$

and the peak gain may also be expressed as

$$G_{peak} \cong \frac{N_{00} \sigma_g R_2 R_p}{D_1} \left(\frac{2}{3} t_{peak} - \frac{1}{D_{a2}} \right) - \alpha_l, \tag{11}$$

where α_l is absorption coefficient, which is proportional to the neutral atom density. Equation (10) indicates that the time needed for the onset of the peak gain is dependent only on the characteristics of lasing medium such as the atom density, electron-impact ionization cross section, Auger decay rate, and the ratio of the statistical weights. As shown in Sec. II, once the laser gain gets its peak value, the pumping of x-ray source almost makes no contribution to the gain because the rate of electron-impact ionization increases more rapidly. Therefore, the time t_{peak} together with the peak gain may be used as a good criterion to select the neutral atom density, laser pulse duration, and the intensity of the driving USP laser. Figure 5 shows the time-varying laser gain calculated via Eq. (9) compared to that of our numerical simulations. It can be seen that the results agree well with each other.

Using Eqs. (10) and (11), we can make a simple estimation on the time t_{peak}, the peak gain, and the requirements on the intensity of the driving USP laser. For a driving USP laser with an energy of 1 J, 40 fs, the IRPR is fit as 2.85

$\times 10^{-6}$ fs^{-2}. The neutral carbon atom density is set as 1.3 $\times 10^{19}$ cm^{-3}, the average electron thermal velocity is selected as 100 eV [13], and the electron-impact ionization cross section of $2p$ may be found in Ref. [15], thus the deduced time t_{peak} is about 41.6 fs, the net peak gain is about 0.5 cm^{-1}, which agrees well with the result of our numerical simulations shown in Sec. II but is much lower than that of Moon and Eder [13]. The cause may be that they have not considered the energy-level split of the upper state $1s^{-1}2s^22p^2$ (^2P,^4P) and thus a higher neutral atom density of 1.0×10^{20} cm^{-3} is used. Moon and Eder therefore overestimated the laser gain. For a driving USP laser with an energy of 100 TW, 20 fs, the IRPR is fit as 6.9×10^{-6} fs^{-2}. The neutral carbon atom density is set as 3.0×10^{19} cm^{-3}, thus the deduced time t_{peak} is about 28 fs, and the net peak gain is about 2.1 cm^{-1}, which agrees well with the result of our numerical simulations shown in Sec. II. The laser gain is proportional to the IRPR as shown in Eq. (11), which means that a rapid increase rate of pumping rate would yield a higher laser gain; the advantage of employing an ultrashort pulse laser is therefore obvious. If the rise time of the pumping rate of the blackbody source corresponds to the pulse duration (generally the rise time is a little bit longer), we can select the optimum atom density to make the time t_{peak} close to the rise time of pumping rate or the pulse duration. If the atom density is too high, t_{peak} is shorter than the rise time of pumping rate. The expected increase of the laser gain cannot be achieved owing to the increased absorption of neutral atoms and some energy of the x-ray source is wasted.

IV. DISCUSSIONS

The analytical calculations and numerical simulations above show that the analytical expressions for the time t_{peak} and peak gain deduced in Sec. III may be used as a good criterion to analyze the laser gain when the lasing medium is irradiated by a fast rise-time broadband x-ray source. The time t_{peak} is only determined by the intrinsic characteristics of the lasing medium, those are neutral atom density, electron-impact ionization, Auger decay, and the ratio of the statistical weights. An allowable increase of atom density is mainly limited by its electron-impact ionization cross section because it is inversely proportional to the latter when t_{peak} keeps the same. Therefore, it seems that the only access to obtain a higher laser gain is to increase the IRPR of x-ray source by employing an USP laser of high power with shorter pulse duration, where the density of atoms can also be increased a little more. That means a shorter pulse laser possesses an obvious advantage over a longer pulse laser.

The model proposed above is also suitable for low Z elements from nitrogen to neon, and may be scaled to higher Z elements from 11 to 20. It is convenient for us to estimate the requirements on the intensity of the USP laser. For neon, which has an Auger decay rate of (2.7 fs)$^{-1}$, the K-shell ionization energy is 867 eV. Because of the closed-shell electrons, it has a small electron-impact ionization cross section. Moreover the removal of one $1s$ electron of neon inner shell gives $1s^{-1}2s^22p^6$ with only one upper laser state ^2S, therefore the total x-ray pumping rate supports the allowed lasing transition and the five energy levels in the analytical model mentioned above reduce to four energy levels. Nevertheless, the above analytical expressions can still be used to analyze the laser gain of neon atom. The fractional ratio (R_1,R_2) of x-ray pumping rate for neon may be set as $R_1=0$, $R_2=1$. On the other hand, the lower laser state is $1S^12s^22p^5$ (^2P), so the ratio of the statistical weights g is 1/3. If the neutral neon atom density is set as 1.0×10^{20} cm^{-3}, the deduced t_{peak} is about 41 fs. So a net effective gain coefficient of 10 cm^{-1} requires the IRPR $>1.86\times 10^{-5}$ fs^{-2}, with times t_{peak} corresponding to the maximum pumping rate of 7.6×10^{-4} fs^{-1}. Using one-half of the peak K-shell cross section (assuming an average photon energy of 1100 eV), a maximum photon flux $>3.8\times 10^{30}$ photons cm^{-2}s^{-1} is required, which corresponds to 6.7×10^{14} W/cm^2 for photons above the K-shell ionization energy. The requirements of x-ray source is close to the estimation of Kapteyn [9]. However, if a driving USP laser with an energy of 100 TW, 20 fs is employed, the requirements will be reduced. For a driving USP laser with an energy of 100 TW, 20 fs, the IRPR is fit as 1.08×10^{-5} fs^{-2}, which is larger than that of carbon (because the K-shell ionization energy of neon is 867 eV. For a dense plasma of 610 eV temperature, the peak emission of the blackbody spectrum is at about 1000 eV, which is much better matched to the neon inner-shell absorption). The neutral neon atom density is set as 2.0×10^{20} cm^{-3}, thus the deduced time t_{peak} is about 29 fs, the net peak gain is about 5.3 cm^{-1}. Using expression (9), the net laser gain as a function of time along with the USP laser, the filtered intensity of x-ray source and the pumping rate of K-shell in neon is calculated. It is shown in Fig. 6 and the net peak gain is 5.2 cm^{-1}.

V. $K\alpha$ X-RAY LASING AT 3.2 NM IN NITROGEN

The nitrogen atom is another attractive candidate to experimentally realize an ISPI x-ray laser. For nitrogen, an x-ray photon creates a K-shell hole in N creating N^+ where an allowable K to L radiative transition can take place yielding a 3.2 nm photon, which is just within the ''water window.'' The removal of one $1s$ electron of nitrogen gives $1s^{-1}2s^22p^3$ with two states ^3S, ^5S, therefore only 3/8 of the total x-ray pumping rate supports the allowed lasing transition. The upper laser state $(1s^{-1})$ ^3S level has a degeneracy of 3 while the lower laser state $(2p^2)$ ^3P level has a degeneracy of 9 (the fine structure of these transitions is smaller than the linewidth of the x-ray transition and can be ignored), thus the ratio of the statistical weights is 1/3. On the other hand, the removal of one $2p$ electron of nitrogen, which is caused by electron-impact ionization, gives $1s^22s^22p^2$ with three states ^3P, ^1D, ^1S, therefore only 3/5 of N_4 supply the lower laser state and the effective ratio of the statistical weights may be set as 1/5. The Auger decay rate of K-shell hole in nitrogen is (7 fs)$^{-1}$ [15], the K-shell ionization energy is 400 eV and the photo- and electron-impact ionization cross section can be found in Refs. [14,16]. Thus the time t_{peak} is about 45 fs if the density of N atoms is

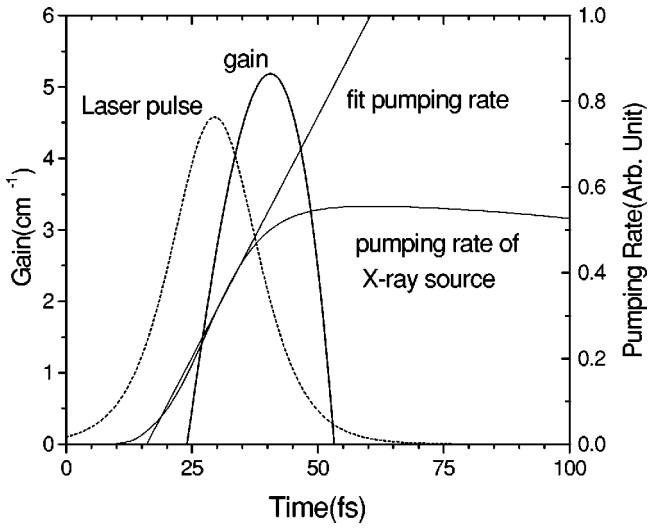

FIG. 6. The net gain of $K\alpha$ x-ray lasing in neon as a function of time calculated via Eq. (9) along with the pumping rate of x-ray source produced by an USP laser of 100 TW, 20 fs.

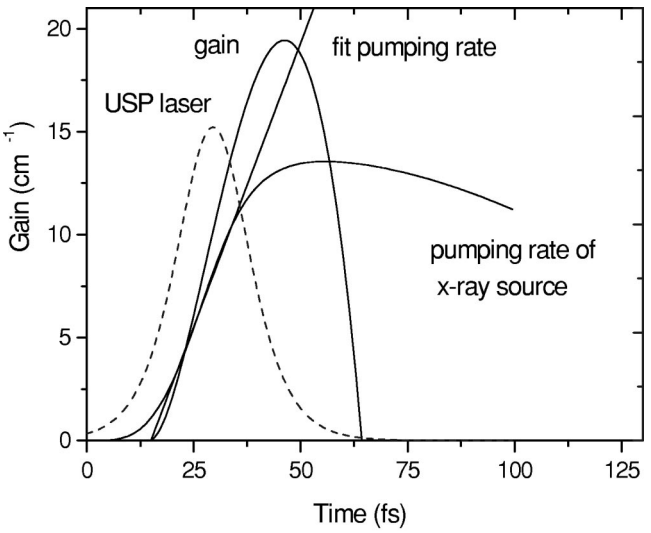

FIG. 7. The gain of $K\alpha$ x-ray lasing in nitrogen as a function of time calculated via Eq. (9) along with the pumping rate of the x-ray source produced by an USP laser of 100 TW, 20 fs.

set as 6.3×10^{19} cm^{-3}. Assuming a net peak gain of 10 cm^{-1}, the IRPR should be $>7.8\times10^{-6}$ fs^{-2}, which times t_{peak} corresponds to the maximum pumping rate of 3.51×10^{-4} fs^{-1}. Using one-half of the peak *K*-shell cross section (assuming an average photon energy of 550 eV), the maximum intensity of x-ray source should be $>1.05\times10^{14}$ W/cm^2 which corresponds to an USP laser of 2.1×10^{17} W/cm^2 if a conversion efficiency of 0.05% of x rays at energies with appreciable *K*-shell cross section is employed.

However, the estimation made above is for the USP laser with a duration of 40 fs. For the current available USP laser of 100 TW, 20 fs [19], using the approximate blackbody model mentioned above, when the laser is focused onto an area of 10 μm$\times$1 cm, we can calculate the pumping rate of *K*-shell photoionization in N atom, which is shown in Fig. 7 along with the fit pumping rate. The rise time of the pumping rate of the x-ray source is about 30 fs and the fit IRPR is $\sim8.9\times10^{-6}$ fs^{-2}. The density of N atoms therefore can be set as 1.3×10^{20} cm^{-3}, the deduced t_{peak} is $\sim$32 fs, and the net peak gain can be calculated as $\sim$13.2 cm^{-1} via Eq. (11) accounting for the absorption of 4.94 cm^{-1}. The laser gain as a function of time calculated via Eq. (9) is also shown in Fig. 7. A gain length product of 13.2 can thus be achieved if the USP laser of 100 TW, 20 fs is employed. On the other hand, the N_2 molecule can be used as a good alternative because the medium density is easy to control. However, owning to the chemical effect of molecular valence, the ratio of the statistical weights increases to 1/2 and the split of vibrational levels in the lower laser state would bring negative effect of linewidth broadening [18]. Thus the intensity of the driving USP laser should be increased a little more. Nevertheless, the negative effect of the N_2 molecule can be compensated by employing a microstructured target [13], which has a high absorption efficiency.

VI. CONCLUSIONS

The model presented in this paper can help us to design the experiments on the ISPI x-ray laser scheme and is convenient for us to analyze the laser gain and estimate the requirements on the intensity of the driving USP laser for different *Z* elements. The success of this scheme is to a large extent dependent on the ability to create an x-ray flash with a rapid rise time. Because the time scale for photopumping and gain lifetime is very short, the travelling-wave laser produced plasma excitation technique would be used to extend the amplification length where the driving ultrashort pulse laser was delayed along the direction of amplification to irridiate the solid target in order to get a travelling-wave x-ray pumping source. It is suggested that $K\alpha$ x-ray lasing at 3.2 nm in nitrogen is an attractive candidate to realize an ISPI x-ray laser. For carbon atom, the *L* shell is an unfilled shell, which makes the level degeneracies less favorable for sustaining an inversion. Moon and Eder overestimated the laser gain [13]. However, for neon atom as mentioned above, the *L* shell is a fully filled shell, which makes the level degeneracies more favorable for sustaining an inversion.

ACKNOWLEDGMENTS

This work was supported by the major basic research project of Chinese Academy of Sciences, the Chinese High-Tech Program, the Chinese National Major Basic Research Development Program, the Chinese National Natural Science Foundation (Contracts No. 19774058 and No. 69925513), and the Shanghai Center for Applied Physics (Contract No. 99JC14006).

[1] C. P. J. Barty, T. Guo, C. Leblanc, F. Rakesi, C. Rosenpetruck, J. Squier, R. R. Wilson, V. V. Yakovlev, and K. Yamakawa, Opt. Lett. **21**, 668 (1996).
[2] M. D. Perry and G. Mourou, Science **264**, 917 (1994).
[3] Ruxin Li, Zhizhan Xu, Tsuneyuki Ozaki, and Hiroto Kuroda, Phys. Lett. A **263**, 117 (1999).
[4] T. Ditmire, J. Zweiback, V. P. Yanovsky, T. E. Cowan, G. Hays, and K. B. Wharton, Nature (London) **398**, 489 (1999).
[5] Ch. Spielmann, N. H. Burnett, S. Sartania, R. Koppitsch, M. Schnurer, C. Kan, M. Lenzner, P. Wobrauschek, and F. Krause, Science **278**, 661 (1997).
[6] M. A. Duguay and P. M. Rentzepis, Appl. Phys. Lett. **10**, 350 (1967).
[7] M. M. Murnane, H. C. Kapteyn, M. D. Rosen, and R. W. Falcone, Science **251**, 531 (1991).
[8] M. M. Murnane, H. C. Kapteyn, and R. W. Falcone, Phys. Rev. Lett. **62**, 155 (1989).
[9] H. C. Kapteyn, Appl. Opt. **31**, 4931 (1992).
[10] M. M. Murnane, H. C. Kapteyn, S. P. Gordon, J. Boker, E. N. Glytsis, and R. W. Falcone, Appl. Phys. Lett. **62**, 1068 (1933).
[11] M. M. Murnane, H. C. Kapteyn, S. P. Gordon, and R. W. Falcone, Appl. Phys. B: Lasers Opt. **58**, 261 (1994).
[12] K. Moribayashi, A. Sasaki, and T. Tajima, Phys. Rev. A **58**, 2007 (1998).
[13] S. J. Moon and D. C. Eder, Phys. Rev. A **57**, 1391 (1998).
[14] H. Tawara and T. Kato, At. Data Nucl. Data Tables **36**, 167 (1987).
[15] E. J. McGuire, Phys. Rev. **185**, 1 (1969).
[16] J. J. Yeh and I. Lindau, At. Data Nucl. Data Tables **32**, 1 (1986).
[17] A. Caruso and R. Gratton, Plasma Phys. **11**, 839 (1969).
[18] L. O. Werme, B. Grennberg, J. Nordgren, C. Nordling, and K. Siegbahn, Phys. Rev. Lett. **30**, 523 (1973).
[19] K. Yamakawa, M. Aoyama, S. Matsuoka, T. Kase, Y. Akahane, and H. Takuma, Opt. Lett. **23**, 1468 (1998).